Serpentinization of Oceanic Peridotites: Implications for Geochemical Cycles and Biological Activity

Gretchen L. Früh-Green, James A.D. Connolly, and Alessio Plas

Institut für Mineralogie und Petrographie, ETH-Zürich, Zürich, Switzerland

Deborah S. Kelley

School of Oceanography, University of Washington, Seattle, Washington, USA

Bernard Grobéty

Institut de Mineralogie et Petrographie, Perolles, Fribourg, Switzerland

Ultramafic rocks are a major component of the oceanic lithosphere and are commonly exposed near and along slow- and ultra-spreading ridges and in other tectonically active environments. The serpentinization of mantle material is a fundamental process that has significant geophysical, geochemical and biological importance for the global marine system and for subduction zone environments. Mineral assemblages and textures are typically complex and reflect multiple phases of alteration, deformation and veining during emplacement, hydrothermal alteration, and weathering. In this paper, we review mineralogical and geochemical consequences of serpentinization processes in oceanic upper mantle sequences in different tectonic environments and discuss the relationship between serpentinization and fluid chemistry. We present phase equilibria that provide models for interpreting mineral-fluid relationships in oceanic serpentinites and allow the simultaneous evaluation of the conditions for redox, hydration and carbonation processes. These models predict that serpentinization reactions are sensitive to Si content of ultramafic rocks and that serpentine phases have an upper stability limit of ~450°C, where H_2O-rich fluids will be dominant. More pervasive serpentinization commences with olivine breakdown reactions below ~425°C and leads to progressively more reduced fluids with decreasing temperature. Our calculations indicate that carbonates may have extensive stability fields in CH_4-rich fluids in Si-deficient systems and that they may be significant in generating reducing conditions. If methane formation driven by serpentinization is common, its contribution to the carbon cycle in submarine biogeochemical systems may be substantial. Serpentinization may thus be an important process in sustaining diverse microbial communities in subsurface and near-vent environments and has consequences for the existence of a deep biosphere.

The Subseafloor Biosphere at Mid-Ocean Ridges
Geophysical Monograph Series 144

10.1029/144GM08

1. INTRODUCTION

Mantle peridotites and lower crustal plutonic rocks are significant components of the oceanic lithosphere. They are exposed on the seafloor in many tectonic settings, such as along fracture zones, at the walls of rift valleys, along non-volcanic passive margins, in subduction zones and in various other tectonic windows in the ocean crust (Figure 1). Variably altered ultramafic rocks are particularly abundant in slow- to ultra-slow spreading ridge environments that are characterized by low magma supply and/or complex tectonic processes related to spreading and strike-slip faulting. In these environments, they may comprise ~20% or more of the oceanic crust [e.g., *Bonatti and Michael*, 1989; *Dick*, 1989; *Cannat*, 1993; *Cannat et al.*, 1995; *Karson*, 1998]. Along the Mid-Atlantic Ridge (MAR), mantle peridotites and associated plutonic rocks occur at the inside corners of ridge-offset intersections or along major faults that bound median valleys. However, they are not restricted to near-ridge discontinuities and segment ends, as exemplified by the MAR 15°N region where they are symmetrically distributed along the axial valley walls [*Cannat and Casey*, 1995; *Lagabrielle et al.*, 1998]. In addition, peridotite-dominated massifs are a common feature at non-transform offsets such as south of the Azores [*Gràcia et al.*, 2000].

The alteration of these rocks is a fundamental process that has significant geophysical, geochemical and biological importance for the global marine system and for subduction zone environments. Hydration of the oceanic mantle during serpentinization processes is accompanied by a decrease in bulk density and a change in rheology that directly affect the strength and physical properties of the mantle, the magnetic and gravity signatures, and the seismic velocities [e.g., *Miller et al.*, 1996; *Hirth et al.*, 1998]. The depth to which serpentinization may occur is controlled by the depth to which seawater can penetrate into the oceanic crust and upper mantle. The depth of circulation will largely be controlled by tectonic processes and fracture permeabilities. Thus, the depth and spatial extent of serpentinization of oceanic peridotites has direct consequences for the interpretation of seismic velocities and may influence where geophysists estimate the position of the seismic Moho. However, more detailed information and particularly drilling into deeper mantle sequences are needed to truly be able to determine if, or in which tectonic environments, the seismic Moho is a hydration boundary.

Serpentinization of olivine in lower crustal and upper mantle lithologies is associated with the uptake and release of many major and minor elements, such as H_2O, Mg, Ca, Si, Cl and B, which has important consequences for long-term global geochemical fluxes. In addition to the production of heat through exothermic reactions, serpentinization leads to reduced, high pH fluids with high H_2 and CH_4 concentrations. A close association between serpentinization processes and elevated volatile contents is indicated by an increasing number of discoveries of H_2 and CH_4 anomalies in the water column above ultramafic outcrops on the MAR [e.g. *Charlou et al.*, 1991a,b; *Rona et al.*, 1992; *Bougault*,

Slow- and ultra-slow spreading ridges:
(1) Mid-Atlantic Ridge (MAR)
(2) Cayman Trough
(3) SW-, SE- and Central Indian Ridges
(4) American-Antarctic Ridge

Intermediate to fast-spreading ridges:
(5) Garrett Fracture Zone
(6) Mathematician Ridge, Hess Deep and Ecquador Fracture Zone

Passive margins:
(7) Spitsbergen margin
(8) Iberian margin and Gorringe Bank
(9) SW Australian margin

Arc-subduction environments:
(10) Mariana and Izu-Bonin forearcs
(11) Tonga Trench
(12) Puerto Rico Trench
(13) Tyrrhenian Sea (ODP Site 651)
(14) South Sandwich arc-basin

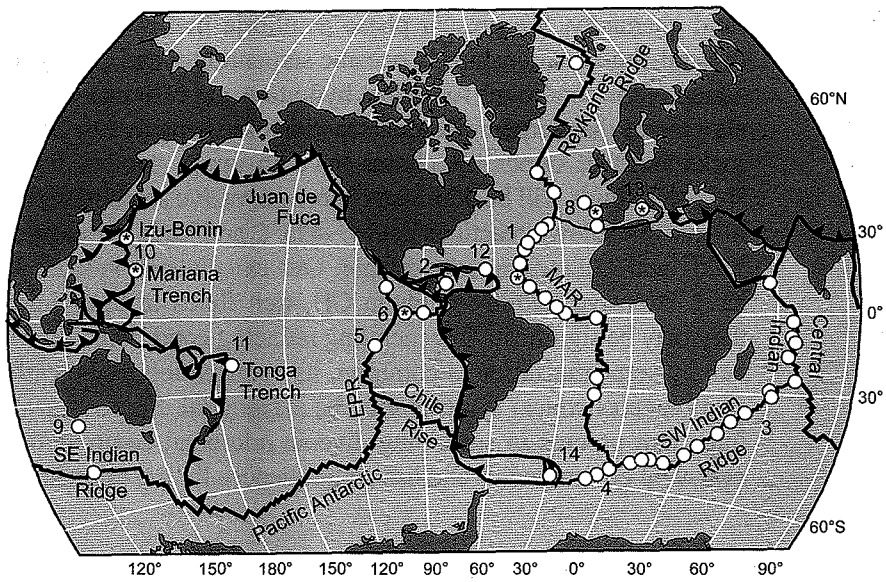

Figure 1. Distribution of oceanic peridotites recovered by dredging, drilling or by submersible in various tectonic settings. Occurrences sampled during ODP drilling legs are shown with stars. For more detailed descriptions and references, see *Bonatti and Michael* [1989]; *Dick* [1989]; *Cannat* [1993]; *Lagabrielle et al.* [1998]; *Gràcia et al.*, [2000]; *Pearce et al*, [2000].

et al., 1993; *Charlou and Donval*, 1993; *Gràcia et al.*, 2000]. The recent discovery of the peridotite-hosted, Lost City hydrothermal field near the MAR at 30°N has particularly intensified the interest in understanding the role of serpentinization in controlling fluid chemistries and in driving hydrothermal flow in off-axis environments [*Kelley et al.*, 2001; *Lowell and Rona*, 2002]. In addition to promoting carbonate and Mg-hydroxide deposition, the relatively cool, alkaline fluids at the Lost City vent field support dense microbial communities that include anaerobic thermophiles [*Kelley et al.*, 2001]. Viewed in this context, the production of volatiles during serpentinization may thus be an important process in sustaining diverse microbial communities in subsurface and near-vent environments and may be significant for the existence of a deep biosphere.

In this paper, we review serpentinization processes in oceanic upper mantle sequences. We discuss the relationship between serpentinization and fluid chemistry and examine the role of serpentinization in the production of highly reduced, volatile-rich fluids and condensed hydrocarbons. Our discussion draws on data from serpentinites from Hess Deep in the equatorial eastern Pacific Ocean, the transverse Ridge of the Vema Fracture Zone in the Atlantic Ocean, the Atlantis Massif east of the MAR at 30°N, the Tyrrhenian Sea, and the Conical and Torishima Seamounts in the western Pacific Ocean [*Früh-Green*, 1995; *Früh-Green and Plas*, 1995, *Früh-Green et al.*, 1996; *Plas*, 1997; *Plas and Früh-Green*, 1998; *Früh-Green et al.*, unpublished data], and compares these results with other published studies. We also present calculations of phase equilibrium in altered peridotites that provide models for interpreting phase relations in oceanic serpentinites and allow the simultaneous evaluation of the conditions for redox, hydration and carbonation processes.

2. ALTERATION OF OCEANIC PERIDOTITES

2.1. Mineralogical and Chemical Consequences

Oceanic peridotites have been sampled by dredging, drilling and submersibles from numerous localities along the mid-ocean ridge system, at ocean-continent transitions, and in subduction zone environments (Figure 1). Fresh mantle peridotites are extremely rare. Nearly all samples are moderately to highly (40-100%) serpentinized and are characterized by mineralogical and textural variations related to the progressive (commonly static) hydration of the primary minerals olivine (Ol), orthopyroxene (Opx) and clinopyroxene (Cpx) during interaction with seawater at decreasing temperatures [e.g. *Prichard*, 1979; *Kimball et al.*, 1985; *Hébert et al.*, 1990; *Früh-Green et al.*, 1996; *Mével and Stamoudi*, 1996; *Dilek et al.*, 1997]. The textures and mineral assemblages are complex and reflect multiple phases of alteration, deformation and veining during emplacement, hydrothermal alteration, and late-stage, low temperature alteration and weathering (Figure 2).

Early phases of hydration are marked by the alteration of primary Opx to form talc- and/or (Ca, Mg) amphibole-bearing ± chlorite assemblages (commonly at temperatures >500°C) or by bastite serpentine textures consisting of lizardite ± chlorite ± magnetite ± FeNi alloys. Alteration to amphibole-bearing assemblages at temperatures greater than 600°C is relatively rare and has been reported from the Islas Orcas Fracture Zone in the South Atlantic [*Kimball et al.*, 1985] and from peridotites drilled at Site 651 during Leg 107 of the Ocean Drilling Program (ODP) in the Tyrrhenian Sea (a back-arc basin related to subduction) [*Bonatti et al.*, 1990; *Plas*, 1997].

Serpentinization is dominated by the progressive alteration of olivine to lizardite- and/or chrysotile-bearing assemblages that form characteristic mesh-textured pseudomorphs. A number of mineralogical, petrographical and textural studies of oceanic serpentinites show that in the early stages of serpentinization, platy lizardite replaces olivine in concentric shells to form serpentine mesh cores (Figure 3a) [*Prichard*, 1979; *Hébert et al.*, 1990; *Früh-Green et al.*, 1996; *Mével and Stamoudi*, 1996; *Dilek et al.*, 1997]. Lizardite may occur together with Fe-rich brucite ± magnetite ± chlorite ± FeNi alloys (+ rare antigorite or calcite). Brucite-bearing assemblages can form reddish brown mesh cores that may be misinterpreted as clay-bearing assemblages in thin section [e.g. as falsely reported in *Früh-Green et al.*, 1996]. Serpentinization reactions commonly continue after olivine is completely consumed and are characterized by the replacement of lizardite ± brucite with chrysotile and magnetite ± sulphide assemblages along mesh rims and as fibers filling micro-veins (Figures 3a,b). Replacement of an early lizardite-brucite-FeNi alloy assemblage by chrysotile + magnetite is particularly well developed in the Hess Deep serpentinites, and as discussed below, may indicate changes in fluid composition with progressive serpentinization. The formation of talc ± tremolite ± chlorite assemblages can accompany serpentinization (e.g. at the Lost City vent field) and may be related to metasomatic reactions and Si-Al transport during interaction of seawater with mafic rocks within the oceanic peridotites.

The occurrence of magnetite, FeNi alloys and other native metals in serpentinized peridotites has received considerable attention because of the importance of Fe-rich phases in producing reducing conditions and in catalyzing the formation of abiogenic methane [e.g. *Frost*, 1984; *Peretti et al.*, 1992; *Horita and Berndt*, 1999]. Few studies of oceanic peridotites include detailed mineralogical characterization of the FeNi phases. *Frost* [1984] indicates that the compositional range

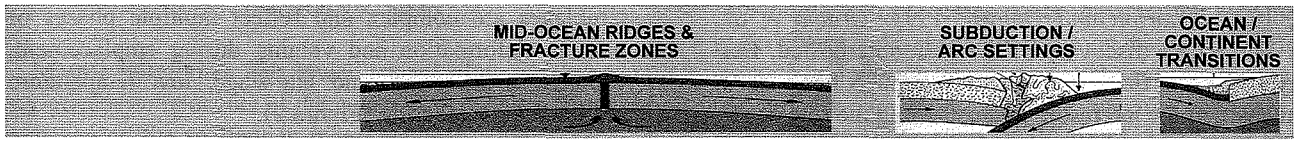

	Hess Deep	MAR 21°N/ MARK	Vema FZ N. Atlantic	Atlantis FZ Lost City Vent Field	Tyrrhenian Sea	Mariana / Izu-Bonin Forearc	Iberian Margin
ODP | Legs	147	109, 153			107	125	103, 149, 173
Characteristic Alteration Minerals:							
Ca-Mg Amphibole	●	●	●	●	●		
Talc	●	●		●	●		
Antigorite (<1%)	●	●				●	
Lizardite	●	●	●	●	●	●	●
Chrysotile	●	●	●	●	●	●	●
Brucite	●	●	●	●	?	●	
Chlorite	●	●	●	●	●	●	●
Taenite (FeNi Alloy)	●	n.d.[a]		n.d.		n.d.	
Magnetite	●	●	●	●	●	●	●
Clay			●	●	●	●	●
Characteristic Deformation:							
Shearing		●	●	●	●	●	●
Fracturing / Veining	●	●	●	●		●	●
Brecciation / Carbonation				●		●	●
Boron (ppm) in:							
Serpentine	30-50	n.d.	20-130	n.d.	60-160	n.d.	30-60
Brucite	40-60	n.d.	n.d.	n.d.		n.d.	
Amphibole	n.d.	n.d.	19	n.d.	n.d.	n.d.	
Clay (palygorskite)			≥200	n.d.	>200	n.d.	n.d.
Chlorine (avg. wt%)							
Serpentine	0.15		0.3	0.7	0.5		0.4
Bulk Carbon (ppm)	275-780	520-1360	30-100	n.d.	570-1470	190-1180	110-780
$\delta^{13}C_{Bulk}$ (‰ VPDB)	-12 to -4	-27 to -26	-27 to -22	n.d.	-23 to -9	-28 to -12	-28 to -20
$\delta^{18}O$ Serpentine (‰ VSMOW)	2.1 to 5.1	2.5 to 4.5 [b]	1.7 to 6.4 [c] 5.7 to 7.5 [d]	2.7 to 5.5	3.0 to 7.8	5.5 to 7.4 [e] 6.0 to 12.4 [f]	2.8 to 14.2
T of Serpentinization [g]	350-400° [h]	350-450° [h]	bimodal [i]	>200°	250-300°	bimodal [j]	100-150°

Figure 2. Summary of characteristic alteration minerals, deformation features, B, Cl, bulk C concentrations and isotopic signatures of oceanic peridotites from different tectonic settings. Notes: [a]n.d. = not determined or not reported; [b]data from *Agrinier and Cannat* [1997]; [c]porphyroclastic peridotites; [d]mylonitic peridotites; [e]serpentinite clasts and [f]serpentine matrix in serpentinite seamounts (includes range of data from *Sakai et al.*, [1990]); [g]approximate temperature range (°C) of serpentinization; [h]temperatures based on serpentine-magnetite ^{18}O thermometry. Bimodal O-isotope compositions reflect different temperature ranges: [i]T~200-350°C and T~150-250°C; [j]T~150-250°C and T~<150°C.

of FeNi alloys in serpentinites lies between approximately 60 and 90 wt% Ni. Although awaruite, the FeNi phase with an ordered crystal structure, is likely most common in serpentinites (Figure 4), transmission electron microscopy (TEM) analyses of the Hess Deep samples documented for the first time in oceanic serpentinites the presence of taenite, the high-temperature FeNi phase with a disordered structure [*Grobéty et al.*, 1997; *Plas*, 1997].

In contrast to regionally metamorphosed alpine serpentinites in ophiolites, the high-temperature serpentine phase antigorite is rare in oceanic peridotites. In oceanic rocks, antigorite is generally restricted to veins and shear zones or as submicroscopic intergrowths in the olivine pseudomorphs [*Prichard*, 1979; *Hébert et al.*, 1990; *Früh-Green et al.*, 1996; *Plas*, 1997]. TEM studies of the Hess Deep serpentinites indicated that antigorite is a minor component of the early lizardite-brucite-taenite assemblages in the mesh cores, and when present, forms intergrowths with the surrounding lizardite [*Grobéty*, 2003 *in press*]. Antigorite was also found locally together with chrysotile forming veinlets that rim, or crosscut the serpentine mesh textures. Analytical electron microscopy (AEM) and coregistered TEM studies on the Hess Deep serpentinites indicated that chrysotile is poorer in Fe and richer in Mg than antigorite or lizardite (Figure 3c) and that high Al-contents are restricted to submicroscopic intergrowths of chlorite. The changes in mineral assemblages and serpentine chemistry can be related to changes in oxygen fugacity and element activities (e.g. Si, Fe and Mg) and may not necessarily reflect major changes in temperature (Figure 3b).

Multiple generations of veins are common in oceanic serpentinites and document processes of brittle deformation and fluid infiltration throughout the metamorphic-tectonic histories of the oceanic sequences (Figure 3a). Hydration

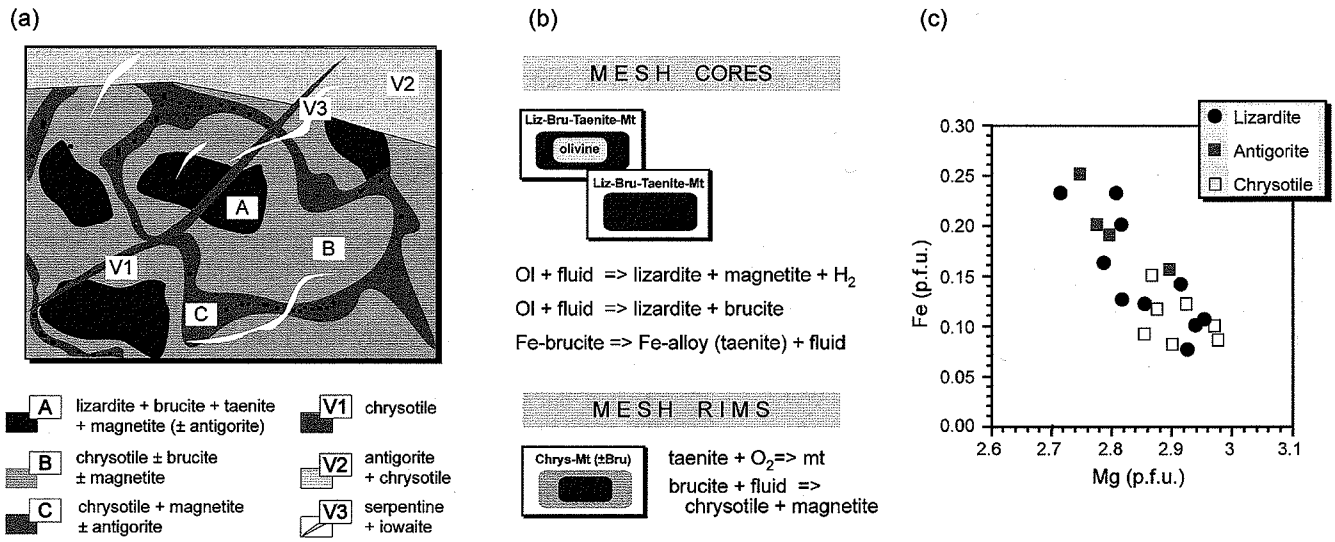

Figure 3. (a) and (b) Schematic diagrams of mineral assemblages and textures during progressive serpentinization (based on petrographic and TEM studies of Hess Deep serpentinites). The changes in mineral assemblages and serpentine chemistry can be related to changes in oxygen fugacity and element activities (e.g. silica and magnesium) rather than to major changes in temperature. (c) AEM data showing varying Fe- and Mg-contents among the serpentine polymorphs in samples from Hess Deep. Compositions have been normalized to a serpentine stoichiometry of $(Mg,Fe)_3\ Si_2O_5\ (OH)_4$ and are given as per formula unit (p.f.u.) relative to this stoichiometry.

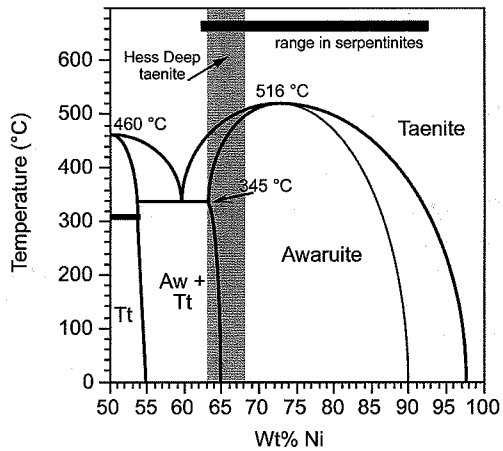

Figure 4. FeNi-alloy phase diagram [after *Reuter et al.*, 1988]. At high temperatures, Fe-Ni phase equilibria is dominated by taenite (γ-phase), a disordered phase with a FCC-structure. Alloys with very high Ni-content (>95 wt%) retain the FCC-structure down to room temperature. Taenite with Ni-contents between 65 and 95% is transformed into the ordered phase, awaruite (Aw; γ'-phase) characterized by a primitive lattice and a doubling of the cell edges relative to the disordered phase. Alloys with 50 to 55 wt% Ni transform into an ordered tetragonal structure below 320°C (γ''-phase, tetrataenite =Tt). The stability of the γ''-phase is disputed. Some published phase diagrams show no stability field for the γ''-phase, but a γ' + α-phase field, where the α-phase represents an iron-rich alloy with BCC structure (kamacite). The horizontal bar shows the range of Fe-Ni alloys in serpentinites [after *Frost*, 1985]; the vertical shaded region shows the composition range of taenite in the Hess Deep samples.

expansion during serpentinization may also be a significant processes in creating successive episodes of microfractures and in propagating cracks [*Macdonald and Fyfe*, 1985]. Vein-filling minerals associated with the main serpentinization events include lizardite, chrysotile, tremolite, chlorite, magnetite, diopside, talc, antigorite, and brucite; whereas fibrous chrysotile ± magnetite are most common [*Prichard*, 1979; *Hébert et al.*, 1990; *Fryer et al.*, 1990; *Früh-Green et al.*, 1996; *Mével and Stamoudi*, 1996; *Dilek et al.*, 1997]. The ubiquitous nature of serpentine-filled microveins further attests to the fact that serpentinization is a continuous process in the oceanic lithosphere and is related to multiple

phases of fracturing and infiltration of seawater. Veining during late-stage, low temperature alteration is generally dominated by the precipitation of aragonite (and/or calcite), brucite, Mg-rich clay minerals, zeolites, and iowaite. Iowaite and similar magnesium iron-hydroxychloride phases (belonging to the pyroauite-sjögrenite group minerals) are particularly abundant in late-stage veins in the Hess Deep serpentinites [*Plas*, 1997] and have been found in serpentine muds recovered from two seamounts in the Mariana and Izu-Bonin forearcs during ODP Leg 125 [*Heling and Schwarz*, 1992]. These brucite-like minerals contain up to 7wt% Cl and may be an important sink for seawater chlorine in serpentinizing fluids.

Low temperature overprinting and weathering of serpentine assemblages is marked by the presence of Mg-rich clays minerals (predominantly smectite, sepiolite and palygorskite), Fe-oxides, hydroxides, and carbonate minerals [*Schmitz et al.*, 1982; *Bonatti et al.*, 1983; *Karpoff et al.*, 1989]. Oxygen isotope analyses of late-stage aragonite in veins and serpentine matrix consistently indicate ambient seawater temperatures (<10°C). These data indicate that seawater-peridotite interaction and mineral precipitation continues long after pervasive serpentinization has occurred [*Bonatti et al.*, 1980; *Sakai et al.*, 1990; *Agrinier et al.*, 1995; 1996; *Früh-Green et al.*, 1996]. However, wall rock alteration associated with late stage veining is commonly lacking or is restricted to the direct vicinity of the vein. The recent studies of *Snow and Dick* [1995] on abyssal peridotites and *Gibson et al.* [1996] on peridotites drilled from the Galicia Margin during ODP Leg 149 suggest that low temperature alteration and carbonation of oceanic serpentinites may result in a loss of Si and Mg and could have a significance influence on global geochemical budgets. For example, it has been estimated that Mg loss from submarine ultramafic material may be as high as 85% of the yearly Mg flux for rivers [*Snow and Dick*, 1995].

In addition to Cl, serpentine assemblages are enriched in B compared to unaltered rocks and B-contents tend to increase with increasing degree of alteration [*Thompson and Melson*, 1970; *Bonatti et al.*, 1984; *Plas*, 1997]. In a study using Secondary Ion Mass Spectrometry (SIMS) analysis, *Plas* [1997] documented high B-concentrations of 30-160 ppm in five oceanic serpentinite samples from different tectonic settings. The results showed that brucite and clay minerals, such as palygorskite, may incorporate higher quantities of boron than serpentine and that serpentine veins and veinlets may contain similar or higher boron than rock serpentine with no compositional gradients toward the wallrock (Figure 2). In contrast to earlier studies of *Bonatti et al.* [1984], the study of *Plas* [1997] showed no direct correlation between B-content and O-isotope temperature and that high B contents were observed in samples formed at high temperature. The results of *Plas* suggest that other parameters, such as fluid/rock ratio, mineralogy, and/or fluid chemistry likely play a major role in determining the amount of boron in ocean floor serpentinites.

2.2. *Temperatures of Serpentinization*

Fundamental to understanding the processes of serpentinization is the determination of the depth and temperature of seawater penetration. These two parameters are also important because they may shed light on the relative timing of serpentinization in the overall tectonic history of ocean basins, but admittedly they are difficult to constrain. The stable isotope geochemistry of modern oceanic rocks, in particular, has been used to monitor processes of fluid-rock interaction and allows the extent and temperatures of seawater circulation and the possible interaction between high-temperature metamorphism and late-stage magmatic processes to be inferred.

Serpentinites from different tectonic settings are characterized by highly variable $\delta^{18}O$ values and negative δD values that are commonly interpreted as indicating a large range of alteration temperatures, variable fluid-rock ratios and possibly the presence of a deuterium-depleted hydrothermal fluid [*Wenner and Taylor*, 1973; *Hébert et al.*, 1990; *Sakai et al.*, 1990; *Agrinier et al.*, 1995; 1996; *Früh-Green et al.*, 1996; *Agrinier and Cannat*, 1997; *Plas and Früh-Green*, 1998; *Früh-Green*, unpubl. data). As discussed above, local alteration of pyroxene can occur at temperatures greater than 600°C [*Kimball et al.*, 1985; *Plas*, 1997]. In contrast, pervasive serpentinization of olivine predominately occurs in multiple stages below temperatures of approximately 350°-400°C, with local overprinting and veining down to nearly ambient seawater temperatures. Comparison of our studies with published data indicate that a bimodal distribution of oxygen isotope signatures, which reflect both high (>~300°C) and low (<~250°C) temperature phases of alteration, is common in oceanic serpentinites. This bimodal distribution is typically related to differences in deformation structures, such as the presence or absence of preexisting mylonite zones or zones of pervasive brecciation (Figure 2). Comparison of serpentinites from over ten localities indicates that serpentinization above ~300°C may be common in ridge environments where heat flow is high. In contrast, low temperature serpentinization below 150°-200°C, characterized by ^{18}O-enriched isotopic signatures with $\delta^{18}O$ values up to 13‰ (VSMOW), is more typical in passive margin and subduction zone settings (Figure 2).

Estimates of serpentinization temperatures are generally difficult to make because equilibrium conditions may rarely be attained in oceanic peridotites, and because multiple phases of alteration and varying PH_2O are common. The temperatures at which oceanic mantle lithologies are altered

depend greatly on primary mineral modes and fluid chemistries. Thermodynamic constraints on phase equilibrium (see below) predict that high temperature serpentinization is sensitive to Si content and modal percentage of Opx. They also predict that at pressures less than ~2 kbar, more dunitic-rich compositions will not be serpentinized until the shallow mantle sequences have cooled to temperatures below ~425°C, when olivine breakdown reactions commence and serpentine + magnetite are thermodynamically stable or below ~350° where serpentine + brucite are stable [e.g. *Evans and Trommsdorff*, 1970]. In fact, experimental data of *Martin and Fyfe*, [1970] suggest that maximum reaction rates for the hydration of olivine at low fluid/rock ratios may occur at temperatures of ~250°C, which is significantly lower than the equilibrium temperatures at which olivine begins to alter to serpentine. On the basis of permeability experiments, *Macdonald and Fyfe* [1985] conclude that oceanic serpentinization is a relatively rapid process and they estimate that at 300°C, a 1km thick layer of serpentinite can form in approximately 1 Ma. Constraints on relative serpentinization temperatures can also be made through the determination of the ordered/disordered nature of FeNi alloys and their Ni-contents (Figure 4) [*Frost*, 1985; *Grobéty et al.*, 1997]. For example, in the Hess Deep serpentinites, the presence of taenite with nickel contents of 63-68wt% indicate serpentinization temperatures of approximately 350-400°C and are consistent with temperatures calculated from O-isotope compositions of serpentine and magnetite. The fact that taenite is preserved in these rocks also suggests that serpentinization and uplift of the Hess Deep mantle sequences was relatively fast.

3. PHASE EQUILIBRIUM CONSTRAINTS ON SERPENTINIZATION AND FLUID COMPOSITION

Since the earliest studies of alpine peridotites and ultramafic rocks in ophiolites, it has been known that serpentinization occurs under conditions of low oxygen fugacity (fO_2) and results in the generation of hydrogen-rich fluids and native metals [e.g., *Ramdohr*, 1967; *Coleman*, 1967; *Barnes et al.*, 1972; *Moody*, 1976; *Frost*, 1985; *Peretti et al.*, 1992]. The formation of hydrogen-rich fluids during serpentinization is attributed to the production of magnetite during olivine hydration and is generally described by simplified model reactions with Fe end-member phases. In reality, serpentinization involves a series of continuous metastable reactions governed by local variations in the activities of elements, particularly Si, Mg, Fe, Ca, C and H^+ in the fluid. Oxygen fugacity (fO_2) is controlled by processes of fluid-rock interaction and is typically determined by reactions among magnetite, Fe-alloys, silicate minerals and potentially carbonates. In the following sections, we examine the relationship between redox conditions and serpentinization during fluid-rock interaction on the basis of thermodynamic models of graphite-saturated ultramafic systems. The constraint of graphite-saturation provides a limiting model for serpentinization reactions that circumvents the necessity of making arbitrary assumptions about the values of unknown potentials such as oxygen fugacity and carbon activities. Conditions at, or close to, graphite saturation are consistent with observations of methane anomalies associated with ultramafic outcrops on the seafloor, with recent experimental studies, and carbon concentration and isotope analyses in oceanic gabbroic and peridotite sequences (discussed below).

3.1. Computational Details

In contrast to more conventional models based on arbitrarily defining fluid activities or mineral buffers, we present phase relations as a function of fluid composition, X_O, the atomic fraction of oxygen relative to hydrogen; $X_O \equiv n_O/(n_O + n_H)$, where n_O and n_H are the number of moles of oxygen and hydrogen, respectively [*Labotka*, 1991; *Connolly*, 1995]. In a graphite-saturated C-O-H fluid, X_O is directly proportional to the fO_2 of carbon (graphite)-saturated C-O-H fluids, and because X_O can only be affected by fluid-rock interaction, it is an ideal measure of redox conditions. By thermodynamic projection of the C-O-H fluid composition through carbon into the O-H subcomposition, carbon-saturated systems can be described by a binary O-H fluid with the compositional variable X_O [*Connolly*, 1995]. The advantage of describing the fluid by variables related to the proportions of its components rather than by the thermodynamic activities of its species (e.g., fO_2, aH_2O) is that the proportions of the components are independent of processes of internal equilibration, and thus directly reflect mass balance constraints on fluid-rock interaction.

The T-X_O sections shown in Figures 5-7 have been calculated using the computer program described by *Connolly* [1990] for a pressure of 1 kbar and for graphite-saturated C-O-H systems, taking into consideration the phases shown in Figure 6. Phases written in lower case are modeled as stoichiometric compounds; those capitalized are modeled as ideal Fe-Mg solutions. Thermodynamic data for all minerals, with the exception of serpentine, were taken from a revised version of *Holland and Powell's* [1990] database. Since no thermodynamic data is available for lizardite, antigorite data were used as a proxy for all serpentine minerals and were derived using the constraints discussed by *Trommsdorff and Connolly* [1990].

3.2. C-O-H-S Fluid Speciation as a Function of X_O

The significance of X_O is demonstrated by the isobaric-isothermal C-O-H phase diagram shown in Figure 5a

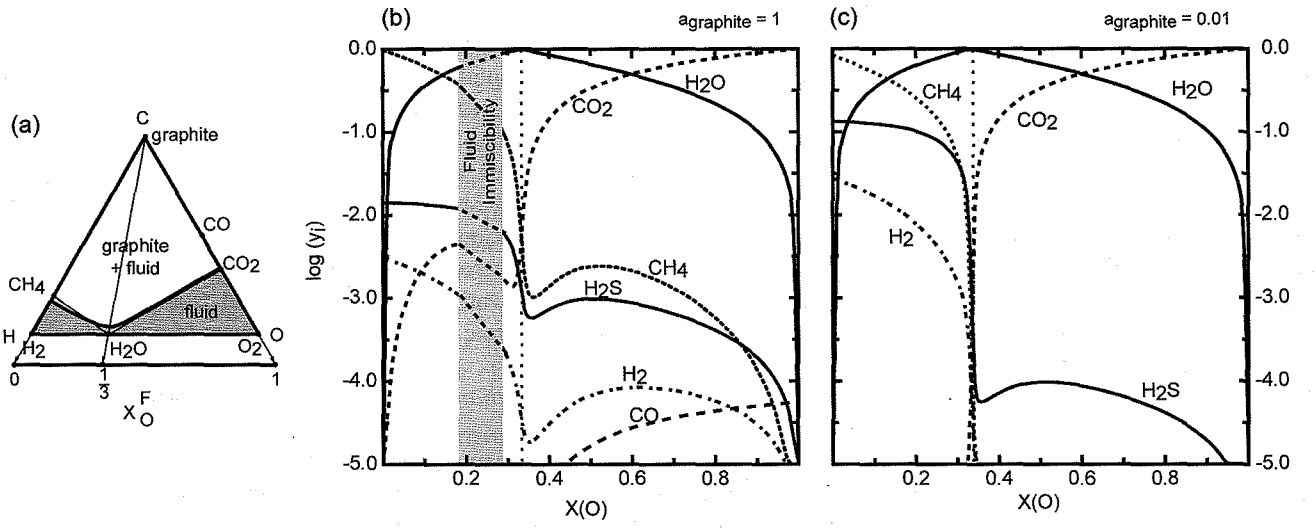

Figure 5. (a) Schematic isobaric-isothermal composition phase diagram for the C-O-H system illustrating the relation between X_O and carbon-saturated C-O-H (GCOH) fluid compositions. Figures b and c show the mole fraction (y_i) of fluid species as a function of X_O in C-O-H-S fluids, calculated for 350°C, 1 kbar and sulphur fugacities corresponding to the pyrite + pyrrhotite buffer for (b) graphite-saturated and (c) graphite-undersaturated conditions. Vertical dotted lines mark the X_O = 1/3 composition (H_2O).

[*Connolly*, 1995]. The possible compositions of a C-O-H fluid that coexists with graphite lie along the boundary between the two-phase field in which graphite coexists with a fluid and the one-phase field (shaded region in Figure 5a) for carbon-undersaturated fluids. The boundary between these fields is the carbon-saturation surface. The composition of a C-O-H fluid coexisting with graphite (i.e., a GCOH fluid) corresponds to the point on the carbon-saturation surface intersected by a line drawn from the graphite composition through the bulk composition of the system. Only H_2, CH_4, H_2O, CO, CO_2 and O_2 are present in significant amounts in GCOH fluids, together with H_2S when sulphur is added to the system (GCOHS) [*Holloway*, 1984; *Connolly*, 1995]. Here we define reducing and oxidizing conditions relative to the redox state of a fluid formed by the reaction of water with graphite (i.e., X_O = 1/3). This convention differs from the common practice of defining redox conditions relative to an arbitrary fO_2 buffer such as nickel nickel-oxide (NNO) or quartz magnetite fayalite (QFM). Thus, in our terminology an X_O < 1/3 fluid is reducing, but such a fluid may in fact be oxidizing relative to QFM (Figure 7).

In Figure 5b, we show the results of computed changes in mole fraction (y_i) of the fluid species H_2, CH_4, H_2O, CO, CO_2 and H_2S as a function of X_O of GCOHS fluids ($a_{graphite}$ = 1) for 350°C, 1 kbar and sulphur fugacities corresponding to the pyrite + pyrrhotite buffer. At conditions of X_O < 1/3, typical of serpentinization reactions in oceanic peridotites (see Figures 6 & 7), H_2O and CH_4 are the dominant fluid species. Methane is the most abundant species at X_O < ~0.14. For graphite undersaturated conditions, (e.g., $a_{graphite}$ = 0.01, Figure 5c), CH_4, H_2, and H_2S remain significant fluid species at conditions of X_O < ~1/3, but their concentrations decrease rapidly across the X_O = 1/3 boundary. Under both graphite-saturated and -undersaturated conditions, CO_2 is the most abundant fluid species at conditions of X_O > 0.6. Water is the dominant species at X_O = 1/3. Except in the vicinity of the X_O =1/3 composition, GCOH fluids are nearly binary CH_4-H_2O and H_2O-CO_2 mixtures [*Holloway*, 1984; *Connolly*, 1995]. This feature persists for significant degrees of graphite undersaturation.

3.3. *Ultramafic Model Systems*

The systems C-O-H-Fe-MgO-SiO_2 or C-O-H-Fe-MgO-CaO-SiO_2 are common models for interpreting phase relations of altered ultramafic rocks and they provide constraints on redox conditions during hydroxylation and carbonation reactions in oceanic peridotites. In Figure 6 we show computed isobaric T-X_O sections of phase equilibria for all possible bulk compositions in the model C-O-H-Fe-MgO-SiO_2 system at a pressure of 1 kbar. For comparison, Figure 7a shows the results of computed phase equilibria for a fixed, representative, dunite bulk composition and Figure 7b shows isobaric T-X_O sections for a representative harzburgite composition in the model C-O-H-Fe-MgO-CaO-SiO_2 system. In the sections in Figure 7, the shaded (di-variant fields) and white regions (tri-variant fields) represent continuous reactions that cause changes in mineral compositions and modal abundances. Univariant phase fields and invariant points, shown by the thick lines and filled circles,

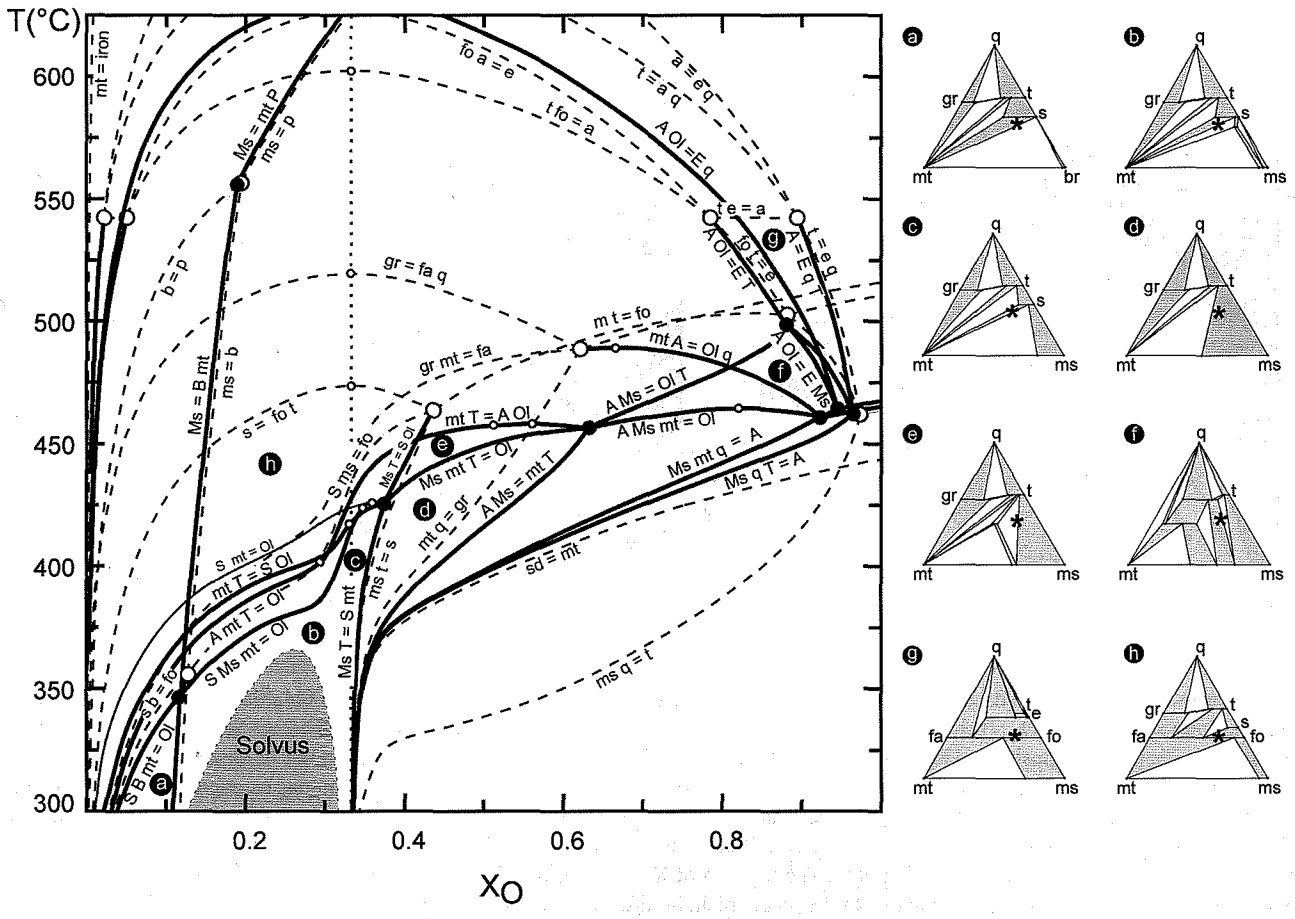

Ideal Fe-Mg solutions

A	anthophyllite	$(Fe,Mg)_7Si_8O_{22}(OH)_2$
B	brucite	$(Fe,Mg)(OH)_2$
Cpx	clinopyroxene	$Ca(Fe,Mg)Si_2O_6$
E	enstatite	$(Fe,Mg)SiO_3$
Ms	magnesite	$(Fe,Mg)CO_3$
P	periclase	$(Fe,Mg)O$
Ol	olivine	$(Fe,Mg)_2SiO_4$
S	serpentine	$(Fe,Mg)_{48}Si_{34}O_{85}(OH)_{62}$
T	talc	$(Fe,Mg)_3Si_4O_{10}(OH)_2$
Tr	tremolite	$Ca_2(Fe,Mg)_5Si_8O_{22}(OH)_2$

Stoichiometric compounds

a	anthophyllite	$Mg_7Si_8O_{22}(OH)_2$	ms	magnesite	$MgCO_3$
b	brucite	$Mg(OH)_2$	mt	magnetite	Fe_3O_4
cc	calcite	$CaCO_3$	p	periclase	MgO
dol	dolomite	$CaMg(CO_3)_2$	q	quartz	SiO_2
e	enstatite	$MgSiO_3$	s	serpentine	$Mg_{48}Si_{34}O_{85}(OH)_{62}$
fa	fayalite	Fe_2SiO_4	sd	siderite	$FeCO_3$
fo	forsterite	Mg_2SiO_4	t	talc	$Mg_3Si_4O_{10}(OH)_2$
gr	grunerite	$Fe_7Si_8O_{22}(OH)_2$			

Figure 6. Calculated isobaric T-X_O phase diagram sections for all possible bulk compositions in the carbon-saturated C-O-H-Fe-MgO-SiO_2 system for a pressure of 1 kbar. Phases denoted by lower case letters are stoichiometric compounds; those capitalized were modeled as ideal Fe-Mg solutions. The position of X_O = 1/3 composition is shown by the vertical dashed line and the position of the GCOH solvus is shown as lightly shaded region. The dashed curves represent stable equilibria in the C-O-H-Fe-SiO_2 and C-O-H-MgO-SiO_2 subsystems; small open circles locate extremum points. Solid curves represent stable C-O-H-Fe-MgO-SiO_2 equilibria and invariant reactions; large open and filled circles are invariant points. The thin, solid grey curve represents the singular curve separating two olivine eutectoidal decomposition reactions. High temperature assemblages are given on the right of the = sign. Circled letters locate conditions for calculated chemographic relations shown at the right. In the chemographic diagrams, filled circles identify compounds; shaded regions are two phase fields. The stars locate a characteristic dunite bulk composition.

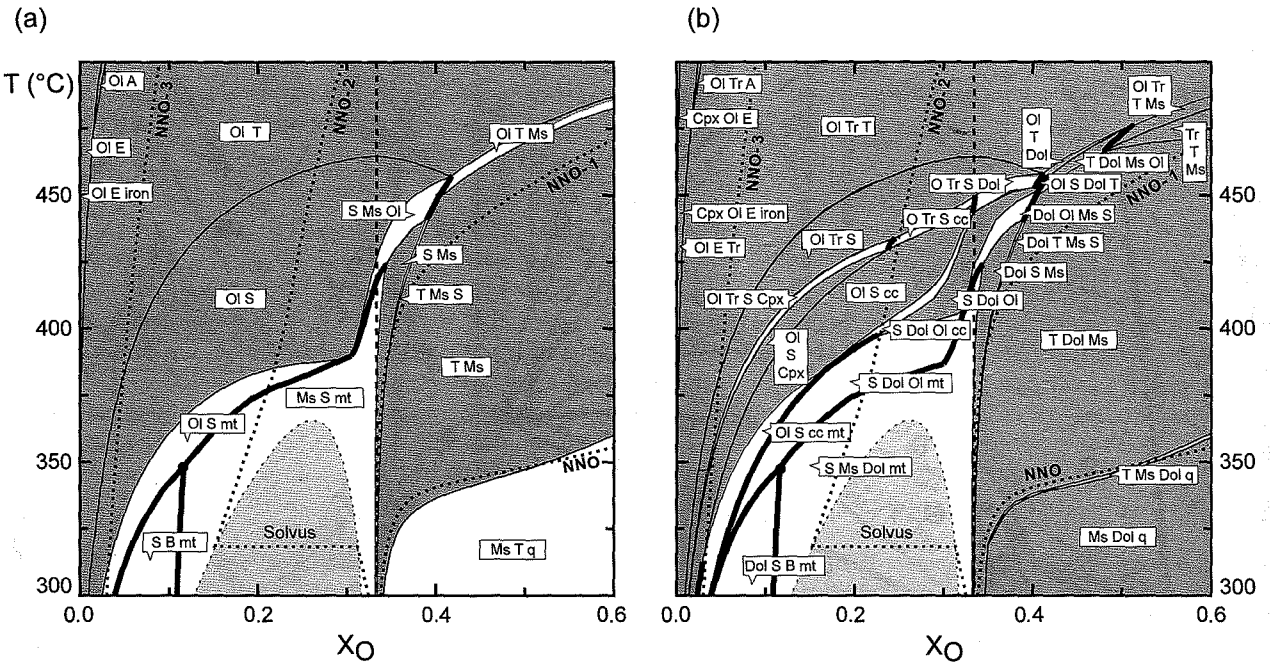

Figure 7. Isobaric T-X_O sections (1kbar) calculated for (a) the carbon-saturated C-O-H-Fe-MgO-SiO_2 system for a fixed, representative dunite bulk composition (39.64 wt% SiO_2, 10.15 wt% FeO, and 47.39 wt% MgO) and (b) for the C-O-H-Fe-MgO-CaO-SiO_2 system for a representative harzburgitic bulk composition (43.79 wt% SiO_2, 8.99 wt% FeO, 43.97 wt% MgO and 1.15 wt% CaO). The shaded and white regions denote the tri- and divariant phase fields defined by continuous equilibria shown in the outlined boxes. Continuous reactions within these fields result in changes in mineral compositions and modal abundances. The thin curves represent extremely narrow divariant fields. Univariant phase fields and invariant points are shown by thick lines and filled circles, respectively. Discontinuous reactions across the univariant curves result in the appearance or disappearance of one phase. The position of X_O = 1/3 composition is shown by the dark, vertical dashed line. The thin dotted lines show the oxygen fugacity relative to the nickel nickel-oxide buffer (NNO), where the number indicates the deviation in log units from NNO (e.g., NNO-3 corresponds to 3 log units below the NNO buffer). Phase notations as shown in Figure 6.

respectively, represent discontinuous phase changes whereby phases appear or disappear. Reaction paths can vary, but in general serpentinization corresponds to conditions of $X_O \leq 1/3$, or oxygen fugacities $\leq$ 1 log unit below NNO (Figure 7). GCOH fluid properties change abruptly across the X_O = 1/3 composition and this may cause anomalous behavior, particularly at low temperature when non-ideality in the fluid species becomes pronounced. This non-ideality effect accounts for the inflections in the univariant fields in the vicinity of the low X_O GCOH fluid solvus.

These models predict that serpentinization reactions are sensitive to Si content of ultramafic rocks and that serpentine-bearing assemblages have an upper stability limit of ~450°C, at which condition the fluid will be H_2O-rich. More pervasive serpentinization commences at temperatures of approximately 425° to 375° C with univariant olivine breakdown reactions (solid lines in Figure 6 and dark lines in Figure 7) that generate progressively more reduced fluids with decreasing temperature. Ultimately serpentinization may result in the formation of brucite-bearing assemblages at approximately 350°C, and corresponds to highly reducing conditions with a maximum X_O of 0.11. Fluid compositions of X_O = 0.11 to 0.19 (depending on temperature) also define the maximum stability of taenite (not shown in Figure 7) at 1 kbar. In silica-deficient systems, such as dunitic and harzburgitic bulk compositions, magnetite-bearing assemblages have a maximum stability close to X_O = 1/3. However, the magnetite stability field may expand significantly in graphite-undersaturated systems, and/or by incorporating Cr. Similarly, Ni may be important in stabilizing iron-alloys. Redox reactions involving iron-alloys may play a major role in controlling fluid chemistry in carbon-free serpentinites. As shown by the positions of the iron phase fields in the far left of Figures 6 and 7, Fe-rich native metals (and Fe-rich alloys) indicate the presence of extremely hydrogen-rich fluids in graphite-saturated systems.

An important feature demonstrated by the diagrams in Figure 7 is that carbonates may have extensive stability fields in methane-rich fluids in silica deficient systems. Carbonate precipitation may in fact be significant in generating reducing fluids during serpentinization as they consume significantly more oxygen than the formation

of magnetite (for every mole of calcite or magnesite (Ms) produced, one mole of oxygen is consumed). The calculated phase equilibria for the harzburgite composition shown in Figure 7b suggests that calcite-serpentine assemblages are stable to more reducing conditions (e.g. at 300°C, X_O = ~ 0.03) than serpentine-brucite assemblages (X_O = ~ 0.05). These calculations also suggest that dolomite is stable under more oxidizing conditions than calcite and should be part of the alteration assemblages below temperatures of approximately 350°C and fluid compositions of X_O > ~0.03. The extensive stability of carbonates in CH_4-rich fluid compositions is due to the dampened variation in the fluid component activities in the vicinity of the GCOH solvus. This effect is only observed at low to moderate pressure, as is relevant for near-ridge serpentinization processes, because with increasing pressure, the equilibria shift to higher temperature relative to the solvus. Thus, for example, by pressures of ~5 kbar, the invariant point defining brucite (b) + magnesite (Ms) + magnetite (mt) + periclase (p) equilibria shifts to the X_O =1/3 fluid composition, and carbonate stability is effectively restricted to oxidized fluid compositions. Because CH_4 and H_2O are the dominant species of reduced GCOH fluids, in terms of species, carbonation reactions are best represented by the general reaction [Connolly, 1995; Holloway, 1984]: $MO + 2H_2O + 2C = MCO_3 + CH_4$, where M represents divalent cations, typically Ca, Mg or Fe.

For graphite activities < 1, carbonate stability is reduced and Fe-Ni alloy stability is expanded for fluid compositions with X_O < 1/3. In this case, the fluids will be characterized by lower bulk H-contents but higher H_2/CH_4 ratios. Thus, the fact that carbonate phases other than calcite are rarely present in oceanic serpentine mineral assemblages, or are restricted to late veins, suggests that either serpentinization occurs at lower temperatures than those considered here or that the carbon activities relevant for oceanic serpentinization are somewhat less than required for graphite saturation. In addition, at pressures lower than 1 kbar, the solvus widens, leading to more extreme fluid compositions.

3.4. Heat Production During Serpentinization

In addition to controlling fluid compositions, serpentinization is commonly believed to generate a significant amount of heat through exothermic hydration. A direct consequence of the thermodynamic models presented above is that the enthalpic changes during serpentinization can be evaluated. Since serpentinization is primarily a hydration process, the enthalpic effect is directly proportional to the amount of water consumed. In the temperature and pressure range considered for our models, the average enthalpy of hydration is 40kJ/mol H_2O (or 2.2kJ/g H_2O). Oceanic serpentinites typically contain 10 to 13 wt% H_2O and have densities in the range of 2.5 to 2.9 g/cm^3. Thus, serpentinization consumes an average of ~300 kg of H_2O/m^3 rock and produces ~6.6 x 10^8 J/m^3 (~2.6 x10^5 J/kg). If we consider the specific heat of an average serpentinized peridotite of ~2.5 x 10^6 J/K/m^3 and discount heat transport, then this heat effect is capable of raising the rock temperature by ~260°C during serpentinization. Enthalpic effects of this magnitude were used in the heat balance models of *Lowell and Rona* [2002]. Their results show that when heat flow and reaction rates are taken into consideration, exothermic serpentinization reactions are capable of driving hydrothermal systems with a wide range of venting temperatures. However, they conclude that low flow rates, high serpentinization rates or additional heat sources, or a combination of these effects, are required to produce high hydrothermal temperatures similar to those observed in basalt-dominated systems.

4. METHANE-RICH FLUIDS IN PERIDOTITE-HOSTED HYDROTHERMAL SYSTEMS

Quantitative data on the composition and nature of H_2- and CH_4-rich fluids generated by alteration of mantle peridotites are scarce; however, recent studies demonstrate that expulsion of CH_4-rich fluids may be of significant importance in chemical and thermal exchanges between the upper mantle and the lithosphere. Large amplitude CH_4 anomalies in the water column above fault-bounded peridotite bodies that exhibit very low total dissolved manganese/methane ratios (TDM/CH_4) confirm that seawater-peridotite interactions generate extensive CH_4 plumes in these crustally thin zones [e.g.; *Jean-Baptiste et al.*, 1991; *Charlou et al.*, 1991 a,b; *Rona et al.*, 1992; *Charlou and Donval*, 1993; *Bougault et al.*, 1993; *Charlou et al.*, 2000]. Additional evidence that significant amounts of CH_4 may be generated during serpentinization is provided by pore waters sampled during ODP Leg 125 at a serpentinized seamount in the Mariana forearc, where high concentrations of CH_4 and C_2H_6 were measured [*Haggerty*, 1989; *Mottl and Haggerty*, 1989]. Seeps that are dominated by CH_4 and H_2 have also been observed emanating from serpentinized bodies in the Zambales ophiolite in the Philippines [*Abrajano et al.*, 1988].

To date, peridotite-hosted hydrothermal fields, characterized by elevated CH_4 and H_2 concentrations, have only been found at the Lost City, Rainbow, Logatchev, and Saldanha sites along the MAR [e.g., *Rona et al.*, 1993; *Barriga et al.*, 1997; *Kelley et al.*, 2001; *Douville et al.*, 2002]. Both the Rainbow and Logatchev fields host black smoker chimneys (350°-360°C) and much of the chemical data (low pH vales, moderate silica, Cu and Zn enrichment) suggest that the vent fluid chemistries are influenced by interaction with gabbroic and basaltic rocks. In contrast, a direct link between serpentinization reactions and hydrothermal venting has been

documented at the Lost City field [*Kelley et al.*, 2001]. Large carbonate-brucite structures appear to be the surface expression of warm (40°-75°C), alkaline (pH 9.0-9.8), Si-poor, and Ca-rich fluids that are emanating from fault zones that tap a region of active serpentinization in the underlying peridotites. Thus, the Lost City field can be considered to represent an end-member hydrothermal system, hosted in peridotites where hydrothermal flow is largely driven by exothermic serpentinization reactions at depth [*Kelley et al.*, 2001].

In addition to serpentinization reactions that produce hydrogen-rich fluids, it is commonly believed that Fischer-Tropsch-type reactions are important for abiotic formation of methane and other hydrocarbons through disequilibrium reactions of CO or CO_2 with H_2, and with FeNi alloys and magnetite as catalysts [e.g. *Yoshida et al.*, 1993; *Berndt et al.*, 1996; *Holm and Charlou*, 2001]. A number of experimental investigations of seawater reaction with ultramafic material at 200°C and 300°C, and 500 bars have shown that CH_4 and H_2 (as well as ethane and propane) occur as reaction byproducts [*Janecky and Seyfried*, 1986; *Berndt et al.*, 1996; *Horita and Berndt*, 1999]. A continuation of these studies by *Allen et al.* [1998] demonstrated that the H_2 reacts with the CO_2-bearing fluids to produce large quantities of formic acid, and smaller concentrations of alkane and alkene gases. However, similar experiments of the reduction of aqueous CO_2 with serpentinized olivine and FeNi alloy + magnetite as catalysts and using labeled ^{13}C, recently conducted by *McCollom and Seewald* [2001], failed to produce significant quantities of methane and none of the other hydrocarbons. *McCollom and Seewald* concluded that although the reactions produced significant quantities of H_2, most of the CH_4 and all of the other hydrocarbons observed in the experiment were derived from a reduced carbon source present in the minerals, rather than from reduction of CO_2 in the fluid. In natural peridotite-hosted systems, it is likely that multiple hydrothermal pulses lead to a residual (reduced) carbon phase in the rocks during fluid-rock interaction and/or through Fischer-Tropsch-type reactions. This residual carbon is then present to react at later times.

The reducing conditions associated with serpentinization have further important consequences for sulphur speciation and mobility. At extremely low oxygen fugacities, serpentinization reactions can lead to the formation of low-sulphur assemblages (e.g. pentlandite+heazlewoodite) with native metals and metal alloys, whereas much more oxidizing conditions may produce higher sulphur assemblages (e.g. pyrite + pyrrhotite ± pentlandite) together with hematite and carbonate minerals [*Eckstand*, 1975; *Frost*, 1985; *Peretti et al.*, 1992; *Alt and Shanks*, 1998]. Based on sulphur isotope data, a recent study of *Alt and Shanks* [1998] on oceanic serpentinites from Hess Deep and the Iberian Margin demonstrated that microbial mediation of sulphate reduction may accompany late-stage serpentinization reactions at low temperatures. Their results suggest that low sulphur contents found at Hess Deep reflect partitioning of sulphur into liquids during partial melting in the mantle and some loss of sulphur during serpentinization at low fluid fluxes, with minimal microbially mediated sulphate reduction. In contrast, low temperature serpentinization under more oxidizing conditions and higher fluid fluxes at the Iberian Margin enhanced microbial seawater sulphate reduction reactions and resulted in a net gain of sulphide.

5. IMPLICATIONS FOR CARBON CYCLES AND BIOLOGICAL ACTIVITY

Preliminary analyses of bulk carbon contents and bulk carbon isotope ratios have been made on samples of serpentinites from different tectonic environments by continuous-flow analysis with a elemental analyzer combined with a ion ratio mass spectrometer (EA-IRMS). Prior to analysis, the samples were decarbonated and degassed at a temperature of 250°C to remove carbonate minerals and surficial contamination, respectively. Our results indicate that up to 1500 ppm carbon may be trapped in oceanic peridotites. In contrast, C-contents of up to 300 ppm were measured in gabbros from slow- and ultra-slow spreading ridges (Figures 2 and 8) [*Früh-Green et al.*, 1996; *Kelley and Früh-Green*, 1999; 2001]. C-isotope analyses of the serpentinite samples from six different regions yielded $\delta^{13}C$ values ranging from -29 to -4‰ and show relatively distinct ranges in $\delta^{13}C$ values for each region (Figure 8). This range of carbon isotope ratios overlap with $\delta^{13}C$ values of oceanic gabbros and span the range of values of carbon in diamonds, alpine peridotites, MOR basalts, and CH_4-rich hydrothermal fluids in some sediment-staved ridges (Figure 9) [see Table 3 in *Kelley and Früh-Green*, 1999]. The range of $\delta^{13}C$ values of the serpentinites are also consistent with C-isotope ratios of methane produced from dissolved bicarbonate in the presence of Fe-Ni alloy in hydrothermal experiments at 300°C [*Horita and Berndt*, 1999]. Interestingly, in regions that have undergone more extensive low temperature alteration (<200°C) and more oxidizing alteration conditions, such as the Vema Transverse Ridge and the Iberian passive margin, carbon concentrations are lower (30 to 350 ppm) and are associated with the more negative $\delta^{13}C$ values (Figure 8). This suggests that late-stage alteration processes under more oxidizing conditions may scavenge carbon from the serpentinites. This interpretation is also supported by S-isotope studies of *Alt and Shanks* [1998].

The presence of significant amounts of carbon is consistent with results from differential thermal/ differential gravimetric analyses (DTA/DTG) and infrared spectroscopy

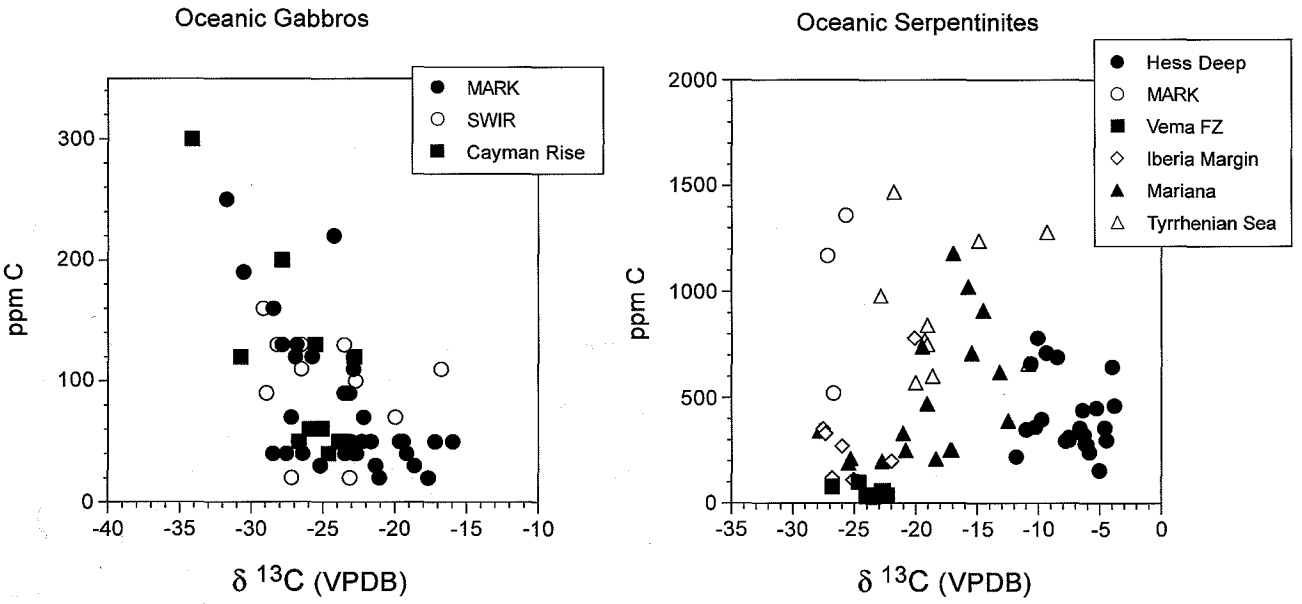

Figure 8. EA-IRMS analyses of bulk carbon content and C-isotope ratios of decarbonated samples of oceanic gabbros and serpentinites from various tectonic environments. Many of the samples are highly depleted in ^{13}C and have corresponding high total C contents. In general, the altered peridotites show up to five times higher total C-concentrations than the oceanic gabbros.

which suggest that the carbon may be present as a condensed phase, possibly as hydrocarbons (*Früh-Green*, unpubl. data). However, as yet, a precise identification of its speciation and its textural relationship to the alteration mineral assemblages has not been possible. Future work is crucial to precisely characterize these species. Studies of mantle hydrocarbons [*Sugisaki and Mimura*, 1994; *Kennedy*, 1995] suggest that unaltered peridotites in ophiolites and peridotite xenoliths contain heavier hydrocarbons (*n*-alkanes from C_{14} to C_{33}), whereas *n*-alkanes are generally lacking in samples that have been serpentinized. However, recent gas chromatograph/mass spectrometer (GC-MS) analyses of fluids from the Rainbow hydrothermal field document the presence of linear saturated hydrocarbons with chain lengths of 16 and 29 carbon atoms [*Holm and Charlou*, 2001] and are consistent with fluid inclusion analyses of the SWIR gabbros which indicated the presence of C_2-C_5 hydrocarbons [*Kelley*, 1996; *Kelley and Früh-Green*, 1999].

Shock [1990; 1992], *McCollom and Shock* [1997] and *Shock and Schulte* [1998] have examined the potential for abiotic synthesis of organic compounds in submarine hydrothermal systems from considerations of thermodynamic data. The results of *Shock and co-workers* demonstrate that conditions are favorable in the oceanic crust for organic synthesis from CO and CO_2 and that the ability to form organic compounds is a strong function of H_2 contents and oxidation states of the fluids [e.g. *Shock*, 1990; 1992; *McCollom and Shock*, 1997; *Shock and Schulte*, 1998; *Zolotov and Shock*; 1999; 2000]. In particular, fluid mixing in hydrothermal systems provides one of the most efficient mechanisms to drive organic synthesis, and, thus, supply geochemical energy to chemolithoautotrophic organisms. The presence of dissolved hydrogen produced through seawater interaction with the oceanic crust and upper mantle provides the reduction potential and the thermodynamic drive for abiotic conversion of CO_2 (or bicarbonate) to organic compounds as hydrothermal fluids mix with seawater. Conversion of CO_2 to hydrocarbon compounds is likely to be most favorable at temperatures below about 500°C because at temperatures greater than this, stable equilibrium appears to be attained and the reduction of CO_2 to CH_4 is kinetically inhibited. At temperatures below ~500°C, at near QFM conditions, metastable equilibrium between CO_2 and aqueous organic compounds may be common in deep-seated submarine environments. The results of *Shock and co-workers* strongly suggest that abiotically produced organic compounds should survive in hydrothermal systems. That hydrothermal systems offer the ideal habitat for the synthesis and preservation of organic compounds has been demonstrated experimentally by *Voglesonger et al.* [2001] who showed that methanol is synthesized from CO_2, H_2 and H_2O under seafloor hydrothermal conditions.

The studies of *Shock and co-workers* and *Voglesonger et al.* [2001] are consistent with recent microbiological studies of samples from the Lost City hydrothermal field which indicate that the relatively cool alkaline fluids support dense microbial communities that occur primarily as microcolonies and isolated cells on the surfaces of carbonate

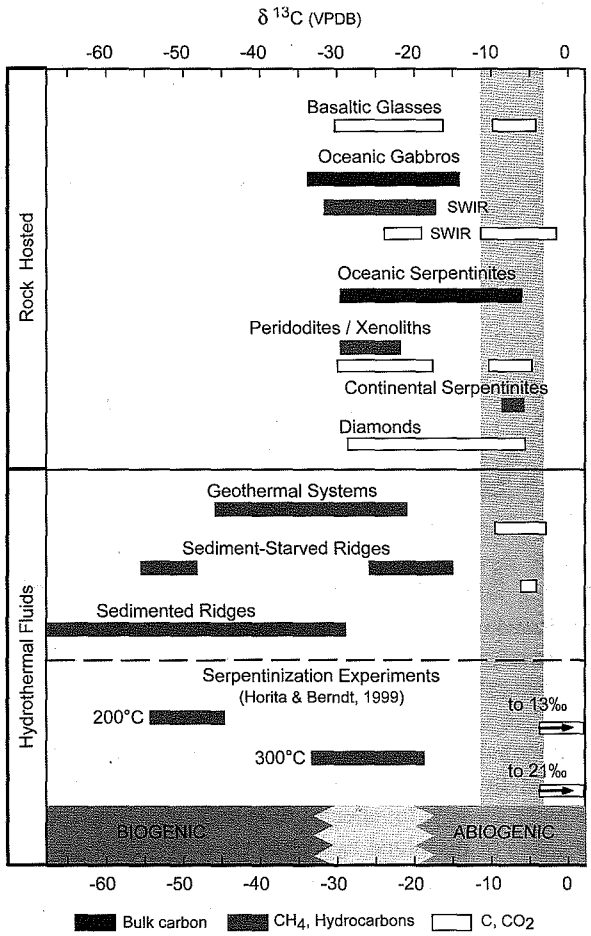

Figure 9. Ranges of carbon isotope ratios ($\delta^{13}C$) of CO_2 (open bars), CH_4 (grey bars) and bulk, non-carbonate bulk carbon (this study) in submarine and geothermal environments [references in Table 3 of *Kelley and Früh-Green*, 1999]. The vertical grey-shaded region represents the range of magmatic CO_2 compositions. $\delta^{13}C$ values of less than -30‰ are generally believed to indicate biogenic processes; however, recent hydrothermal experiments of *Horita and Berndt* [1999] at temperatures of 200°C produced methane with C-isotope ratios that are as low as those typically observed for microbial methane. *Horita and Berndt* conclude that kinetic isotopic fractionations during hydrothermal processes, particularly those related to serpentinization, can produce abiogenic reduced C-species with very low $\delta^{13}C$ values, and thus in such systems, inferences of the origin of methane on the basis of isotopic data may be equivocal.

minerals. Culturing experiments and DNA analyses yielded hyperthermophilic to mesophilic microorganisms of Archaeal and Eubacterial lineages [*Kelley et al.*, 2001]. *Kelley et al.* [2001] conclude that reducing conditions associated with serpentinization of oceanic peridotites may be similar to those of the early Earth. Such systems may have been the requirement for the emergence of life forms on the ocean floor [*Schopf*, 1983; *MacLeod et al.*, 1994; *Russell and Hall*, 1996; *Shock and Schulte*, 1998;]. Similarly, studies of *Holm and Charlou* [2001] on the Rainbow ultramafic hydrothermal fluids suggest that abiotic formation of organic compounds through Fischer-Tropsch type reactions during serpentinization provides an alternative pathway for the formation of early membranes and the origin of life.

6. CONCLUSIONS

In recent years it has become increasingly apparent that geochemical and geological processes in submarine systems are intimately linked with microbial activity and biological diversity. There is now an intense interest in the role of serpentinization processes in crustal aging, in the generation of volatile-rich hydrothermal fluids, and in the biological communities that may be supported in these systems. Present-day serpentinite-hosted environments may be our closest analogue to early Earth systems [*Schopf*, 1983; *Shock and Schulte*, 1998, *Kelley et al.*, 2001; *Holm and Charlou*, 2001] and thus understanding the links between serpentinization reactions and biological processes in oceanic peridotites is of fundamental importance. Because serpentinized peridotites are an important component of the oceanic lithosphere at nearly all tectonic boundaries, these rocks represent a significant reservoir of abiogenic carbon and may support much larger chemosynthetic microbial populations than has previously been believed.

Acknowledgments. We thank Stefano Bernasconi for advice and assistance in carrying out the stable isotope experiments at the ETH, Zürich. The authors appreciate the thoughtful reviews by John Holloway and Peter Saccocia. This work was supported by the ETH-Zürich and Swiss NF (TH 0-20-710-93 and SNF 21-42372.94; Früh-Green) and by NSF under the RIDGE program (OCE-9529 833; Kelley).

REFERENCES

Abrajano, T.A., N.C. Sturchio, J.K. Bohkle, G.L. Lyon, R.J. Poreda, and C.M. Stevens, Methane-hydrogen gas seeps, Zambales ophiolite, Philippines: Deep or shallow origin? *Chem. Geol.*, 71, 211-222, 1988.

Agrinier, P., and M. Cannat, Oxygen isotope constraints on serpentinization processes in ultramafic rocks from the Mid-Atlantic Ridge (23°N), in *Proc. Ocean Drill. Program Sci. Results*, 153, 381-388, 1997.

Agrinier, P., R. Hekinian, D. Bideau, and M. Javoy, Stable isotope compositions ($^{18}O/^{16}O$, D/H, and $^{13}C/^{12}C$) of oceanic crust and upper mantle rocks exposed in the Hess Deep near the Galapagos Triple Junction, *Earth Planet. Sci. Lett.*, 136, 183-196, 1995.

Agrinier, P., C. Mével, and J. Girardeau, Hydrothermal alteration of the peridotites cored at the ocean/continent boundary of the Iberian Margin: Petrologic and stable isotope evidence, *Proc. Ocean Drill. Program Sci. Results*, 103, 225-234, 1988.

Agrinier, P., G. Cornen, and M-O. Beslier, Mineralogical and oxygen isotopic features of serpentinites recovered from the ocean/continent transition in the Iberian Abyssal Plain, *Proc. Ocean Drill. Program Sci. Results*, 149, 541-552, 1996.

Allen, D.A., M.E. Berndt, W.E. Seyfried Jr., and J. Horita, Inorganic reduction of CO_2 to HCOOH, CH_4, and other reduced carbon compounds with application to subseafloor hydrothermal systems (abstract), *Eos Trans AGU*, 79, Fall Meet. Suppl., 58-59, 1998.

Alt, J.C., and W.C. Shanks III, Sulfur in serpentinized oceanic peridotites: Serpentinization processes and microbial sulfate reduction, *J. Geophys. Res.*, 103, 9917-9929, 1998.

Barnes, I., and J.R. O'Neil, The relationship between fluids in some fresh alpine-type ultramafics and possible modern serpentinization, Western United States, *Bull. Geol. Soc. Am.*, 80, 1947-1960, 1969.

Barringa, F.J.A.S., I.M.A. Costa, J.M.R. Relvas, A. Ribeiro, Y. Fouquet, H. Ondreas, L. Parson, and the FLORES Scientific Party, Discovery of the Saldanha Hydrothermal field on the FAMOUS Segment of the MAR (36°30N) (abstract), *Eos Trans AGU*, 79, Fall Meet. Suppl., 67, 1998.

Berndt, M.E., D.E. Allen, and W.E. Seyfried, Jr., Reduction of CO_2 during serpentinization of olivine at 300°C and 500 bar, *Geology*, 24, 351-354, 1996.

Bonatti, E., and Michael, P. J., 1989. Mantle peridotites from continental rifts to ocean basins to subduction zones, *Earth Planet. Sci. Lett.*, 91, 297-311.

Bonatti, E., J. R. Lawrence, P.R. Hamlyn, and D. Breger, Aragonite from deep sea ultramafic rocks, *Geochim. Cosmochim. Acta*, 44, 1207-1214, 1980.

Bonatti, E., E.C. Simmons, D. Breger, P.R. Hamlyn, and J.R. Lawrence, Ultramafic rock/seawater interaction in the ocean crust: Mg-silicate (sepiolite) deposition from the Indian Ocean floor, *Earth Planet. Sci. Lett.*, 62, 229-238, 1983.

Bonatti, E., J.R. Lawrence, and N. Morandi, Serpentinization of ocean-floor peridotites: temperature dependence on mineralogy and boron content, *Earth Planet. Sci. Lett.*, 70, 88-94, 1984.

Bonatti, E., M. Seyler, J. Channell, J. Giraudeau, and G. Mascle, Peridotites drilled from the Tyrrhenian Sea, ODP Leg 107, *Proc. Ocean Drill. Program Sci. Results*, 107, 37-47, 1990.

Bougault, H., J.-L. Charlou, Y. Fouquet, H.D. Needham, N. Vaslet, P. Appriou, P.J. Baptiste, P.A. Rona, L. Dmitried, and S. Silanties, Fast- and slow-spreading ridges: Structure and hydrothermal activity, ultramafic topographic highs, and CH_4 output, *J. Geophys. Res.* 98, 9643-9651, 1993.

Cannat, M., Emplacement of Mantle Rocks in the Seafloor at Mid-Ocean Ridges, *J. Geophys. Res.*, 98, 4163-4172, 1993.

Cannat, M., and J. Casey, An ultramafic lift at the Mid-Atlantic Ridge: successive stages of magmatism in serpentinized peridotites from the 15°N region, in *Mantle and Lower Crust Exposed in Oceanic Ridges and Ophiolites*, edited by R.L.M. Vissers and A. Nicolas, pp. 5-34, Klawer Academic Publishers, The Netherlands, 1995.

Cannat, M., D. Bideau, and H. Bougault, Serpentinized peridotites and gabbros in the Mid-Atlantic Ridge axial valley at 15°37'N and 16°52'N, *Earth Planet. Sci. Lett.*, 109, 87-106, 1992.

Cannat, M., C. Mével, M. Maia, C. Deplus, C. Durand, P. Gente, P. Agrinier, A. Belarouchi, G. Dubuisson, E. Humler, and J. Reynolds, Thin crust, ultramafic exposures, and rugged faulting patterns at the Mid-Atlantic Ridge (22-24°N), *Geology*, 23, 49-52, 1995.

Charlou, J.L., and J.-P. Donval, Hydrothermal methane venting between 12°N and 26°N along the Mid-Atlantic Ridge, *J. Geophys. Res.* 98, 9625-9642, 1993.

Charlou, J.L., H. Bougault, P. Appriou, P. Jean-Baptiste, J. Etoubleau, and A. Birolleau, Water column anomalies associated with hydrothermal activity between 11°40' and 13° N on the East Pacific Rise: Discrepancies between tracers, *Deep Sea Res.*, 38, 569–596, 1991a.

Charlou, J.L., H. Bougault, P. Appriou, T. Nelsen, and P. Rona, Different TDM/CH_4 hydrothermal plume signatures: TAG site at 26°N and serpentinized ultrabasic diapir at 15°05'N on the Mid-Atlantic Ridge, *Geochim. Cosmochim. Acta*, 55, 3209–3222, 1991b.

Charlou, J.L., J.P. Donval, E. Douville, P. Jean-Baptiste, J. Radford-Knoery, Y. Fouquet, A. Dapoigny, M. Stievenard, Compared geochemical signatures and the evolution of Menez Gwen (37°50'N) and Lucky Strike (37°17N) hydrothermal fluids, south of the Azores Triple Junction on the Mid-Atlantic Ridge, *Chem. Geol.*, 171, 49-75, 2000.

Coleman, R.G., Low-temperature reaction zones and alpine ultramafic rocks of California, Oregon and Washington, *U. S. Geol. Surv. Bull.*, 1247, 1-49, 1967.

Connolly, J.A.D., Calculation of multivariable phase diagrams: an algorithm based on generalized thermodynamics, *Am. J. Sci.*, 290, 666–718, 1990.

Connolly, J.A.D., Phase diagram methods for graphitic rocks and application to the system C-O-H-FeO-TiO_2-SiO_2, *Contrib. Mineral. Petrol.*, 119, 94-116, 1995.

Douville, E., J.L. Charlou, E.H. Oelkers, P. Bienvenu, C.F. Jove Colon, J.P. Donval, Y. Fouquet, D. Prieur, and P. Appriou, The Rainbow vent fluids (36°14'N, MAR): the influence of ultramafic rocks and phase separation on trace metal content in Mid-Atlantic Ridge hydrothermal fluids, *Chem. Geol.*, 184, 37-48, 2002.

Dick, H.J.B., Abyssal peridotites, very slow spreading ridges and ocean ridge magmatism, in *Magmatism in the Ocean Basins*, edited by S.D. Saunders and M.J. Norry, *Geol. Soc. Lond., Spec. Publ.* 42, 71-105, 1989.

Dilek, Y., A. Coulton, and S. Hurst., Serpentinization and hydrothermal veining in peridotites at Site 920 in the MARK area (Leg 153), in *Proc. Ocean Drill. Program Sci. Results*, 153, 35-59, 1997.

Evans, B.W., and V. Trommsdorff, Regional metamorphism of ultramafic rocks in the Central Alps. Parageneses in the system CaO-MgO-SiO_2-H_2O, *Schweiz. Min. Pet. Mitt.*, *50*, 481-492, 1970.

Frost, B.R., On the stability of sulfides, oxides and native metals in serpentinite, *J. Petrol.*, 26, 31-63, 1985.

Früh-Green, G.L., Progressive serpentinization of the upper mantle exposed at the Vema Fracture Zone (Equatorial Atlantic) (abstract). *Eos Trans AGU*, 76(46), Fall Meet. Suppl., 695, 1995.

Früh-Green G.L., and A. Plas, Controls and consequences of serpentinisation at plate boundaries. *Proceedings of the International Ophiolite Symposium*, 48-49, 1995.

Früh-Green, G.L., A. Plas, and C. Lécuyer, Petrologic and stable isotope constraints on hydrothermal alteration and serpentinization

of the EPR shallow mantle at Hess Deep (Site 895), *Proc. Ocean Drill. Program Sci. Results*, 147, 255-292, 1996.

Fryer, P., J.A. Pearce, L.B. Stokking, and Shipboard Scientific Party, *Proc. Ocean Drill. Program, Initial Reports*, vol. 125, Ocean Drill. Program, College Station, Texas, 1990.

Garcia, E., J.L. Charlou, J. Radford-Knoery, and L.M. Parson, Non-transform offsets along the Mid-Atlantic Ridge south of the Azores (38°N-34°N): Ultramafic exposures and hosting of hydrothermal vents, *Earth Planet. Sci. Lett.*, 177, 89-103, 2000.

Gibson, I.L., M.O. Beslier, G. Cornen, K.L. Milliken, and K.E. Seifert, Major and trace element seawater alteration profiles in serpentine formed during the development of the Iberia Margin, *Proc. Ocean Drill. Program Sci. Results*, 149, 519-528, 1996.

Grobéty, B., Polytypes and high-order structures of antigorite: A TEM study, *Am. Min., in press*, 2003.

Grobéty, B., Plas, A., and Früh-Green, G.L., Serpentinization temperature of ocean floor peridotites from the Hess Deep rift valley, (abstract), *Terra Abstracts*, 9(1), 549, 1997.

Haggerty, J.A., Fluid inclusion studies of chimneys associated with serpentinite seamounts in the Mariana Forearc. *Proceedings of Second Pan-American Conference on Fluid Inclusions*, 29, 1989.

Hébert, R., A.C. Adamson, and S.C. Komor, Metamorphic petrology of Leg 109, Hole 670A serpentinized peridotites: serpentinization processes at a slow spreading ridge environment, *Proc. Ocean Drill. Program Sci. Results*, 106/109, 103–115, 1990.

Heling, D., and A. Schwarz, Iowaite in serpentinite muds at Sites 778, 779, 780, and 784: a possible cause for the low chlorinity of pore waters, *Proc. Ocean Drill. Program Sci. Results*, 125, 313-323, 1992.

Hirth G., J. Escartin, and J. Lin, The rheology of the lower oceanic crust: Implications for lithospheric deformation at mid-ocean ridges, in *Faulting and Magmatism at Mid-Ocean Ridges, Geophys. Monogr. Ser.*, vol. 106, edited by W.R. Buck, *et al.*, pp. 291-303, AGU, Washington, D.C., 1998.

Holland, R.J.B., and R. Powell, An enlarged and updated internationally consistent dataset with uncertainties and correlations: the system K_2O-Na_2O-CaO-MgO-Mn-FeO-Fe_2O_3-Al_2O_3-TiO_2-SiO_2-C-H_2-O_2, *J. Met. Geol.*, 8, 89-124, 1990.

Holm, N.G., and J.L. Charlou, Initial indications of abiotic formation of hydrocarbons in the Rainbow ultramafic hydrothermal system, Mid-Atlantic Ridge, *Earth Planet. Sci. Lett.*, 191, 1-8, 2001.

Horita J., and M.E. Berndt, Abiogenic Methane formation and isotopic fractionation under hydrothermal conditions, *Science*, 285, 1055-1057, 1999.

Janecky, D.R., and W.E. Seyfried, Jr., Hydrothermal serpentinization of peridotite within the oceanic crust: Experimental investigations of mineralogy and major element chemistry, *Geochim. Cosmochim Acta*, 50, 1357-1378, 1986.

Jean-Baptiste, P., J.L. Charlou, M. Stievenard, J.P. Donval., H. Bougault, and C. Mével., Helium and methane measurements in hydrothermal fluids from the Mid-Atlantic Ridge: The Snake Pit site at 23°N, *Earth Planet. Sci. Lett.*, 106, 17-28, 1991.

Karpoff, A.M., Y. Lagabrielle, G. Boillot, and J. Girardeau, L'authigenèse océanique de palygorskite par halmirolyse de péridotites serpentiniséees (Marge de Galice): ses implications géodynamiques, *C.R. Acad. Sci., Paris*, 308, Serie II, p. 1341-1348, Paris, 1989.

Karson, J.A., Internal structure of oceanice lithosphere: A perspective from tectonic windows, in *Faulting and Magmatism at Mid-Ocean Ridges, Geophys. Monogr. Ser., 106*, edited by W.R. Buck, *et al.*, pp. 177-218, AGU, Washington, D.C., 1998.

Kelley, D.S., Methane-rich fluids in the oceanic crust. *J. Geophys. Res.* 101, 2943-2962, 1996.

Kelley D.S., and G.L. Früh-Green, Abiogenic methane in deep-seated mid-ocean ridge environments: Insights from stable isotope analyses. *J. Geophys. Res.* 104, 10,439-10,460, 1999.

Kelley D.S., and G.L. Früh-Green, Volatiles in mid-ocean ridge environments, in *Ophiolites and Oceanic Crust: New Insights from Field Studies and Ocean Drilling Program*, edited by Y. Dilek, *et al.*, Geological Association of America, Special Paper 349, pp. 327-260, Boulder, Colorado, 2000.

Kelley, D.S., and Früh-Green, G.L., Volatile lines of descent in submarine plutonic environments: Insights from stable isotope and fluid inclusion analyses, *Geochim. Cosmochim. Acta, 2001.*

Kelley, D.S., J.A. Karson, D.K. Blackman, G.L. Früh-Green, D.A. Butterfield, M.D. Lilley, E.J. Olson, M.O. Schrenk, K.K. Roe, G.T. Lebon, P. Rivizzigno, and the AT3-60 Shipboard Party, An off-axis hydrothermal vent field near the Mid-Atlantic Ridge at 30°N, *Nature*, 412, 145-149, 2001.

Kennedy, J.F., Comment on "Mantle hydrocarbons: Abiotic or biotic?" by R. Sugisaki, and K. Mimura. *Geochim. Cosmochim. Acta*, 59, 3857-3858, 1995.

Kimbal, K.L., F.S. Spear, and H.J.B. Dick, High temperature alteration of abyssal ultramafics from the Islas Orcads Fracture Zone, South Atlantic, *Contrib. Mineral. Petrol.*, 91, 307-320, 1985.

Labotka, T.C., Chemical and physical properties of fluids, in *Contact Metamorphism, Reviews in Mineralogy*, edited by D. Kerrick, vol. 26, Mineralogical Society of America, Washington D.C., 43-104, 1991.

Lagabrielle, Y., A.M. Karpoff, and J. Cotten, Mineralogical and geochemical analyses of sedimentary serpentinites from Conical Seamount (Hole 788A): Implications for the evolution of serpentine seamounts, *Proc. Ocean Drill. Program Sci. Results*, 125, 325-342, 1992.

Lagabrielle, Y., D. Bideau, M Cannat, J.A. Karson, and C. Mével, Ultramafic-,mafic plutonic rock suites exposed along the Mid-Atlantic Ridge (10°N-30°N). Symmetrical-asymmetrical distribution and implications for seafloor spreading processes, in *Faulting and Magmatism at Mid-Ocean Ridges, Geophys. Monogr. Ser.*, vol. 106, edited by W.R. Buck, et al., pp. 153-176, AGU, Washington, D.C., 1998.

Lowell, R.P., and P.A. Rona, Seafloor hydrothermal systems driven by the serpentinization of peridotite, *Geophys. Res. Lett., 29*, No. 11, 10.1029/2001GL01411, 2002.

Macdonald, A.H. and W.S. Fyfe, Rate of serpentinization in seafloor environments, *Tectonophysics*, 116, 123-135, 1985.

MacLeod, G., C. McKeown, H.J. Hall, and M.J. Russell, Hydrothermal and oceanic pH conditions of possible relevance

to the origin of life, *Origin Life Evol. Biosphere*, 23, 19-41, 1994.

Martin, B. and W.S. Fyfe, Some experimental and theoretical observations on the kinetics of hydration reactions with particular reference to serpentinization, *Chem. Geol.*, 6, 185-195, 1970.

McCollom, T.M., and E.L. Shock, geochemical constraints on chemolithoautotrophic metabolism by microorganisms in seafloor hydrothermal systems, *Geochim. Cosmochim. Acta*, 61, 4375-4391, 1997.

McCollom, T.M., and J.S. Seewald, A reassessment of the potential for reduction of dissolved CO_2 to hydrocarbons during serpentinization of olivine, *Geochim. Cosmochim. Acta*, 65, 3769-3778, 2001.

Mével, C., and C. Stamoudi, Hydrothermal alteration of the upper mantle section at Hess Deep, *Proc. Ocean Drill. Program Sci. Results*, 147, 293-309, 1996.

Mével, C., M. Cannat, P. Gente, E. Marion, J.M. Auzende, and J.A. Karson, Emplacement of deep crustal and mantle rocks on the west median valley wall of the MARK area (MAR 23°N), *Tectonophysics*, 190, 31-53, 1991.

Miller, D.J., G.J. Iturrino, and N.I. Christensen, Geochemical and petrological constraints on velocity behavior of lower crustal and upper mantle rocks from the fast-spreading ridge at Hess Deep, *Proc. Ocean Drill. Program Sci. Results*, 147, 477-490, 1996.

Moody, J.B., Serpentinization A review, *Lithos*, *9*, 125-138, 1976.

Mottl, M.J., and J.A. Haggerty, Upwelling of Cl-poor, S and C-rich waters through a serpentinite seamount, Mariana Forearc, ODP Leg 125 (abstract), *Eos Trans AGU*, *70*, Fall Meet. Suppl., 1382, 1989.

Pearce, J.A., P.F. Barker, S.J. Edwards, I.J. Parkinson, and P.T. Leat, Geochemistry and tectonic significance of peridotites from the South Sandwich arc-basin system, South Atlantic, *Contrib. Mineral. Petrol.*, 139, 36-53, 2000.

Peretti, A., J. Dubessy, J. Mullis, B.R. Frost, and V. Trommsdorff, Highly reducing conditions during Alpine metamorphism of the Malenco peridotite (Sondrio, northern Italy) indicated by mineral paragenesis and H_2 in fluid inclusions, *Contrib. Mineral. Petrol.*, 112, 329-340, 1992.

Plas, A., Petrologic and stable isotope constraints on fluid-rock interaction, serpentinization and alteration of oceanic ultramafic rocks, Ph.D. thesis, No. 12261, ETH-Zürich, 252 pp., 1997.

Plas, A., and G.L. Früh-Green, Petrologic and stable isotope constraints on serpentinization and alteration of oceanic ultramafic rocks, *Schweiz. Mineral. Petrol. Mitt.*, *78*, 209, 1998.

Prichard, H.M., A petrographic study of the process of serpentinization in ophiolites and the ocean crust, *Contrib. Mineral. Petrol.*, 68, 231–241, 1979.

Ramdohr, P., A widespread mineral association connected with serpentinization, *Neues Jb. Miner. Abh.*, 107, 241-265, 1967.

Reuter, K.B., D.B. Williams, and J.I. Goldstein, Low temperature phase transformations in the metallic phases of iron and stony-iron meteorites, *Geochim. Cosmochim. Acta*, 52, 617-626, 1988.

Rona, P.A., H. Bougault, J.L.Charlou, P. Appriou, T.A. Nelsen, J.H. Trefry, G.L. Eberhart, A. Barone, and H.D. Needham, Hydrothermal circulation, serpentinization and degassing at a rift-valley fracture zone intersection: Mid-Atlantic Ridge near 15°N, 45°W, *Geology*, 20, 783-786, 1992.

Russell, M. J., and J.A. Hall, The emergence of life from iron monosulfide bubbles at a submarine hydrothermal redox and pH front, *J. Geol. Soc. Lond.*, 153, 1-26, 1996.

Sakai, R., M. Kusakabe, M. Noto, and T. Ishii, Origin of waters responsible for serpentinization of the Izu-Ogasawara-Mariana forearc seamounts in view of hydrogen and oxygen isotope ratios, *Earth Planet. Sci. Lett.*, 100, 291–303, 1990.

Schmitz, W., A. Singer, H. Bäcker, and P. Stoffers, Hydrothermal serpentine in a Hess Deep sediment core, *Mar. Geol.*, 46, 17-26, 1982.

Seitz, M.G., and S.R. Hart, Uranium and boron distributions in some oceanic ultramafic rocks, *Earth Planet. Sci. Lett.*, 21, 97-107, 1973.

Shock, E.L., Geochemical constraints on the origin of organic compounds in hydrothermal systems, *Origins of Life Evol. Biosphere.*, 20, 331-367, 1990.

Shock, E.L., Chemical environments of submarine hydrothermal systems. *Origins of Life Evol. Biosphere.*, 22, 67-107, 1992.

Shock E.L., and M.D. Schulte, Organic synthesis during fluid mixing in hydrothermal systems, *J. Geophys. Res.*, 103, 28513-28527, 1998.

Schopf, J.W., *Earths Earliest Biosphere: Its Origin and Evolution*, Princeton University Press, New Jersey, p 1-543, 1983.

Snow, J.E., and Dick H.J.B., Pervasive magnesium loss by marine weathering of peridotite, *Geochim. Cosmochim. Acta*, 59, 4219-4235, 1995.

Sugisaki, R, and K. Mimura, Mantle hydrocarbons: Abiotic or by biotic? *Geochim. Cosmochim. Acta*, 58, 2527-2542, 1994.

Thompson, G., and W.G. Melson, Boron contents of serpentinites and metabasalts in the oceanic crust: Implications for the boron cycle in the oceans, *Earth Planet. Sci. Lett.*, 8, 61-65, 1970.

Trommsdorff, V., and J.A.D. Connolly, Constraints on phase diagram topology for the system CaO-MgO-SiO_2-H_2O-CO_2, *Contrib. Mineral. Petrol.*, 104, 1-7, 1990.

Voglesonger, K.M, J.R. Holloway, E.E. Dunn, P.J. Dalla-Betta, and P.A. O'Day, Experimental abiotic synthesis of methanol in seafloor hydrothermal systems during diking events, *Chem. Geol.*, 180, 129-139, 2001.

Wenner, D.B., and H.P. Taylor, Oxygen and hydrogen isotope studies of the serpentinization of ultramafic rocks in the oceanic environments and continental ophiolite complexes, *Am. J. Sci.*, 273, 207-239, 1973.

Wetzel, L.R., and E.L. Shock, Distinguishing ultramafic from basalt-hosted submarine hydrothermal systems by comparing calculated vent fluid compositions, *J. Geophys. Res.*, 105, 8319-8340, 2000.

Yoshida, T., K. Nishizawa, M. Tabata, H. Abe, T. Kodama, M. Tsuji, and Y. Tamaura, Methanation of CO_2 with H_2-reduced magnetite, *Journal of Material Sci.*, *28*, 1220-1226, 1993.

Zolotov, M.Y., and E.L. Shock, Abiotic synthesis of polycyclic aromatic hydrocarbons on Mars, *J. Geophys. Res.*, 104, 14033-14049, 1999.

Zolotov, M.Y., and E.L. Shock, A thermodynamic assessment of the potential synthesis of condensed hydrocarbons during cooling and dilution of volcanic gases, *J. Geophys. Res.*, 105, 539-559, 2000.

James A.D. Connolly, Institut für Mineralogie und Petrographie, ETH-Zürich, Sonneggstr. 5, CH-8092 Zürich, Switzerland.

Gretchen L. Früh-Green, Institut für Mineralogie und Petrographie, ETH-Zürich, Sonneggstr. 5, CH-8092 Zürich, Switzerland.

Bernarsd Grobéty, Institut de Mineralogie et Petrographie, Perolles, CH-1700 Fribourg, Switzerland.

Deborah S. Kelley, School of Oceanography, University of Washington, Box 357940. Seattle, WA 98195, USA.

Alessio Plas, Institut für Mineralogie und Petrographie, ETH-Zürich, Sonneggstr. 5, CH-8092 Zürich, Switzerland.